Single proton transfer to ^{29,30}P states*

W. W. Dykoski and D. Dehnhard
John H. Williams Laboratory of Nuclear Physics, University of Minnesota, Minneapolis, Minnesota 55455
(Received 21 July 1975)

Differential cross sections were measured for the (^{3}He, d) reaction on ^{28}Si and ^{29}Si at $E_{^3\mathrm{He}}$ = 25 MeV by use of an Enge split-pole spectrometer. Up to 19 point angular distributions for transitions to 12 states in ^{29}P below 6.4 MeV excitation energy and to 66 states in ^{30}P below 8.7 MeV were analyzed in the distorted-wave Born approximation. The optical model parameters required for the distorted-wave Born approximation analysis were obtained from elastic ^{3}He scattering data which were taken on ^{28}Si, ^{29}Si, and ^{30}Si. A number of ^{30}P levels were found to have large components of simple two-particle structure, with one particle in the $2s_{1/2}$ shell and the other either in the $2s_{1/2}$, $1d_{3/2}$, $1f_{7/2}$, or $2p_{3/2}$ shells. Specifically, the states at 6092 and 7048 keV were assigned $J^\pi = 3^-$, $T = 1$ and $J^\pi = 4^-$, $T = 1$, respectively, because they were found to carry a significant fraction of the $(2s_{1/2})(1f_{7/2})$ strength. However, the $T = 0$ components of the $(2s_{1/2})^2_{1^+}$, $(2s_{1/2})(1d_{3/2})_{1^+}$, and $(1d_{5/2})^{-1}(2s_{1/2})^3_{3^+}$ configurations were found to be distributed among a large number of states. Spin assignments were made based on shapes of the angular distributions and analog relations to ^{30}Si states. An estimate of the extent to which the $1d_{5/2}$ proton shell is filled in ^{28}Si and ^{29}Si was extracted.

[NUCLEAR REACTIONS ^{28,29}Si(^{3}He, d), ^{28,29,30}Si(^{3}He, ^{3}He), $E = 25$ MeV; measured $\sigma(E_d, \theta)$, ^{29,30}P deduced levels, l, J, π, T, spectroscopic factors; measured $\sigma(\theta)$, deduced optical model parameters, enriched target.]

I. INTRODUCTION

Nuclei with two particles or two holes or a particle and a hole added to closed shells have been the subject of many investigations (e.g., Refs. 1–4). Many excited states of such nuclei have been interpreted successfully in terms of a simple two-particle model and information on the effective interaction in nuclei has been extracted. We have studied the structure of states of ^{30}P by stripping a proton onto ^{29}Si using the (^{3}He, d) reaction. This reaction is expected to yield information on states which could be interpreted to arise from coupling a neutron and a proton to a ^{28}Si core. Such a simple model might not be applicable to ^{30}P because it is a nucleus in the transition region between rotational and vibrational nuclei. It is, however, possible that ^{30}P states could be interpreted as simple two-particle Nilsson states, a problem that has attracted much attention.[5] In any case, it is clearly of interest to obtain the single-particle transfer strength for proton transfer to ^{30}P states for a comparison with calculated values based on simple and more complex models. In fact, in a study of the ^{29}Si(d, p)^{30}Si reaction[6] an interpretation of many ^{30}Si states was suggested in terms of a simple weak coupling of a $2s_{1/2}$ nucleon to mass 29 states which are known to carry a significant fraction of the single-particle strength. The same interpretation should hold for $T = 1$ states in ^{30}P. However, as we shall see, the $T = 0$ states appear to be more complex. Thus ^{30}P seems to pose the interesting problem of a simple $T = 1$ spectrum coexisting with a complicated $T = 0$ spectrum which might be described best in a deformed shell model.

We have also studied the ^{28}Si(^{3}He, d)^{29}P reaction to confirm the previously observed strong $2s_{1/2}$, $1d_{3/2}$, $1f_{7/2}$, and $2p_{3/2}$ transitions[7] and to measure the extent to which the $1d_{5/2}$ shell is closed in ^{28}Si in comparison with ^{29}Si.

Because ^{29}P and ^{30}P are proton unbound above 2748 and 5600 keV, respectively, the standard (bound state) distorted-wave Born approximation (DWBA) approach cannot be used. However, a comparison of the ^{28}Si(^{3}He, d) reaction with the (d, p) reaction[8,9] to the mirror nucleus ^{29}Si, where the neutron is bound up to 8474 keV, can yield information on the applicability of the modified[10] DWBA which we used for the unbound states.

II. EXPERIMENT

A. Experimental setup

A 25 MeV ^{3}He beam from the Minnesota MP Tandem Van de Graaff accelerator was used. Self-supporting silicon oxide targets of typically 50–100 μg/cm^2 thickness were made by the evaporation technique. These targets were of natural isotopic composition or of "mixed" com-

position (approximately equal amounts of the three isotopes) or enriched in ^{28}Si (99.58%), ^{29}Si (92.0%), and ^{30}Si (95.55%).

Two surface barrier detectors were mounted at $\theta_{lab} = \pm 30^\circ$ on either side of the beam to monitor target thickness, current integration, and beam stability. These monitors were also used to normalize the yield for the measurements at $\theta_{lab} = 0^\circ$ discussed later.

Reaction products were momentum analyzed by use of an Enge split-pole spectrometer.[11] The deuterons and the ^{3}He particles were detected either by photoemulsions (50 μm thick) or by an array of six position-sensitive solid state detectors, each 30 mm long, placed along the focal surface of the spectrometer. Beam defining slits, 2 mm high, limited the height of the beam spot on the target to assure an image height at the focal surface of the spectrometer of safely less than 10 mm, the height of the position-sensitive detectors. The slit width of 1 mm assured that the contribution from the object size to the over-all resolution width was small. For most of the deuteron runs with photoemulsions, absorber foils were used to stop the tritons and ^{3}He particles.

When position-sensitive solid state detectors are used, usually no absorber foils are needed because the energy loss signal from the detector allows an identification of the particles of interest. For most runs the spectrometer entrance aperture widths were set to 2° for the reaction data and to 1° for the elastic scattering experiments.

B. Reaction spectra

Photographic plates were exposed to deuterons from the ^{28}Si(^{3}He, d)^{29}P reaction at 18 angles and from the ^{29}Si(^{3}He, d)^{30}P reaction at 10 angles. Not counting overlap runs, an additional nine angles were taken for the ^{29}Si target and one angle for the ^{28}Si target with solid state position detectors.

A good resolution spectrum [14 keV full width at half maximum (FWHM)] for the ^{28}Si(^{3}He, d)^{29}P reaction taken with the array of position-sensitive solid state detectors is shown in Fig. 1. Most data for this reaction were taken with photographic plates and by use of a thick target resulting in an over-all resolution of 40 keV (FWHM), by far sufficient to resolve the widely spaced levels of ^{29}P.

The ^{29}P spectrum (Fig. 1) shows that the 4341 keV state is very wide due to its large natural

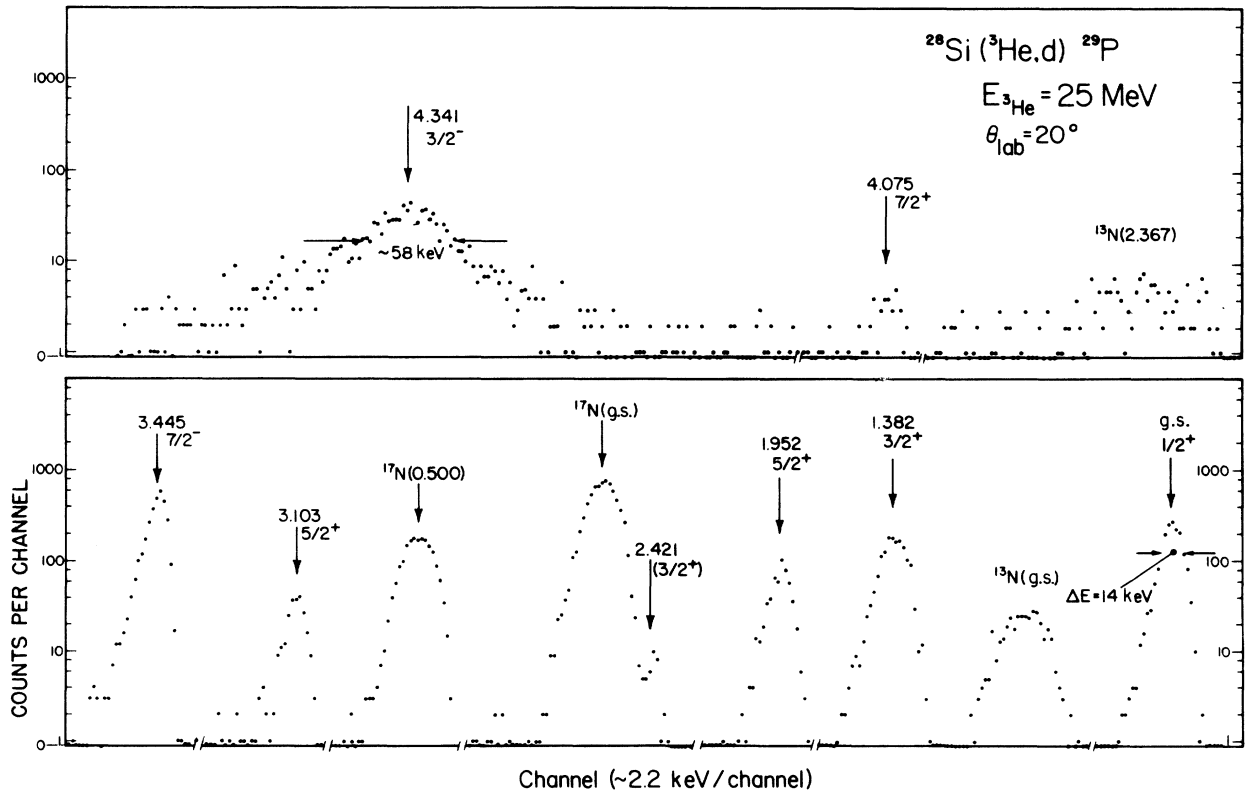

FIG. 1. Spectrum of the ^{28}Si(^{3}He, d)^{29}P reaction at $\theta_{lab} = 20^\circ$ taken with an array of six position solid state detectors. Two overlapping runs are represented and regions with very low background counts are omitted.

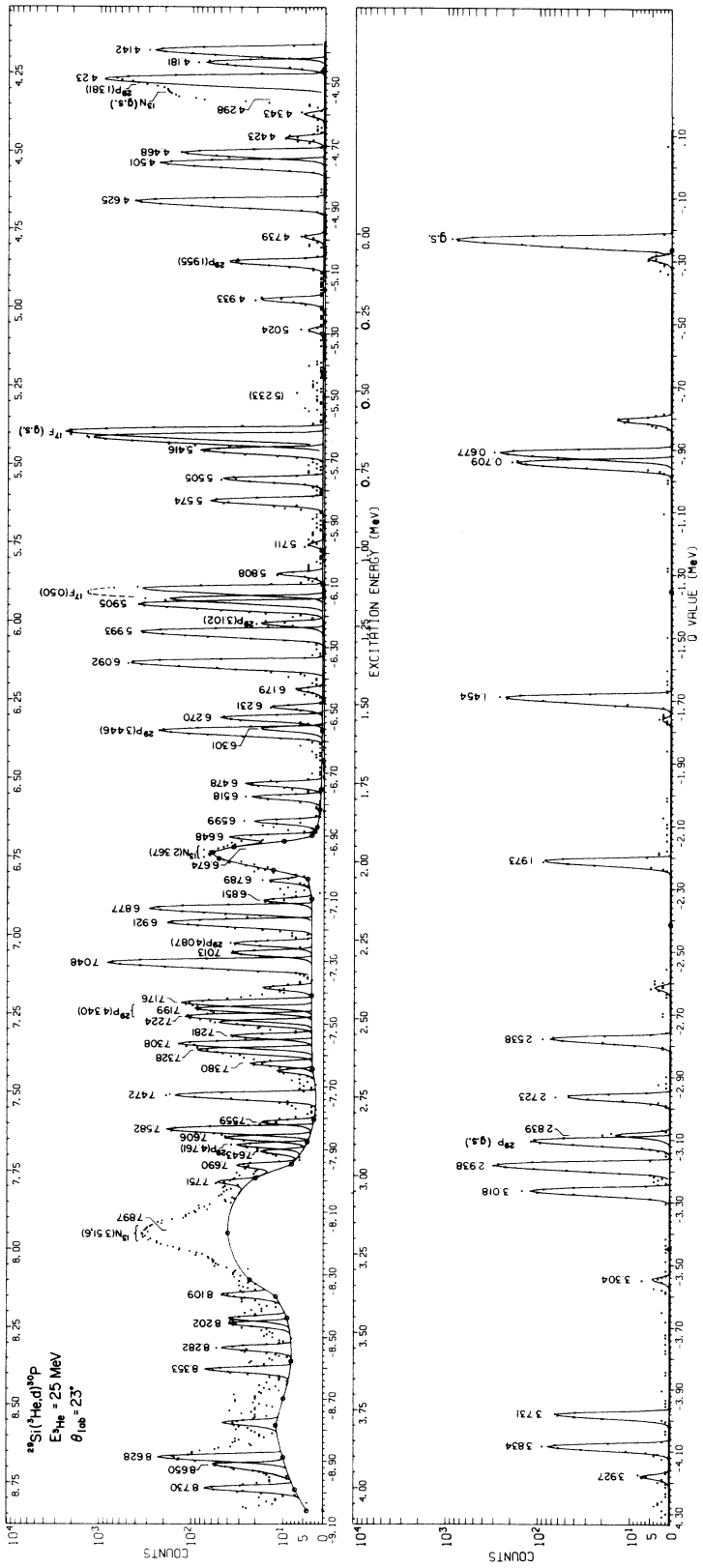

FIG. 2. Spectrum of the ^{29}Si(^{3}He, d)^{30}P reaction at θ_{lab}=23° taken with photographic plates. Absorber foils were not used for this exposure, hence, triton groups are seen, such as the two between the g.s. and the first excitated state of ^{30}P. The peaks were fitted by the computer code AUTOFIT.

TABLE I. Spectroscopic strength $G_j = (2J_f + 1)S$ for single-particle stripping to ^{29}P and ^{29}Si states.

$E_x(^{29}\mathrm{P})$ [a] (keV)	J^π [b]	nlj	G_j for ^{29}P $(^3\mathrm{He}, d)$ [a] at 25 MeV	G_j for ^{29}P $(^3\mathrm{He}, d)$ [c] at 35.3 MeV	(d, n) [c] at 13.48 MeV	$E_x(^{29}\mathrm{Si})$ [b] at (keV)	G_j for ^{29}Si (d, p) [d] at 18 MeV	(d, p) [e] at 10 MeV
0	$\frac{1}{2}^+$	$2s_{1/2}$	1.3	1.0	1.0	0	1.05	1.05
1382± 5	$\frac{3}{2}^+$	$1d_{3/2}$	3.5	2.0	2.2	1273	2.95	2.66
1952± 5	$\frac{5}{2}^+$	$1d_{5/2}$	0.74	0.42	0.54	2028	0.73	1.02
2421± 5	$\frac{3}{2}^+$	$1d_{3/2}$	0.14	···	···	2426	<0.05	···
3103± 5	$\frac{5}{2}^+$	$1d_{5/2}$	0.36	0.06	···	3067	0.35	0.42
3445± 5	$\frac{7}{2}^-$	$1f_{7/2}$	3.7	1.6	2.7	3624	3.0	3.44
4075± 5	$\frac{7}{2}^+$	$1g_{7/2}$	(0.15)	···	···	4080	···	···
4341± 5	$\frac{3}{2}^-$	$2p_{3/2}$	1.7	0.64	0.76	4934	2.25	1.39
4754± 5	$\frac{1}{2}^+$	$2s_{1/2}$	0.06	0.02	···	4840	···	0.05
(5530) [b]	$\frac{1}{2}^-$	$2p_{1/2}$	f	···	···	6381	1.05	0.52
5738± 10	$\frac{5}{2}^-$	$1f_{5/2}$	1.3	0.66	···	6191	1.20	1.48
5967± 10	$\frac{3}{2}^+$	$1d_{3/2}$	0.2	0.04	···	5949	0.25	0.08
6317± 10	$(\frac{9}{2}^+)$ [a]	$1g_{9/2}$	(0.42)	···	···	6770	0.60	···

[a] This experiment.
[b] Reference 12.
[c] Reference 7.
[d] Reference 8.
[e] Reference 9.
[f] State has very large width.

width. $\Gamma_{nat} = (\Gamma_{exp}^2 - \Gamma_{spec}^2)^{1/2}$ was extracted from the data, where Γ_{exp} is the FWHM of the 4341 keV peak and Γ_{spec} is the FWHM of neighboring narrow peaks whose widths were determined by target thickness, beam spot size, spread in the energy of the ^{3}He beam, and spectrometer focal conditions. The resulting $\Gamma_{nat} = 56 \pm 4$ keV is in good agreement with 53 ± 3 keV as listed in Ref. 12, which was obtained from elastic proton scattering on ^{28}Si.

The plates from the ^{29}Si(^{3}He, d)^{30}P reaction were exposed when irradiating a very thin ^{29}Si target. Then a resolution of 15 to 20 keV (FWHM), in best cases of 10 keV, was obtained.

The photoplates for ^{30}P were scanned in 0.25 mm strips and for ^{29}P in 0.5 mm strips, either by eye or by use of the Argonne automatic plate scanning facility. Comparison of results obtained by use of both techniques showed satisfactory agreement. The spectra were analyzed with the computer program AUTOFIT,[13] which automatically locates peaks and yields peak positions and integrated counts in the individual peaks. Figure 2 shows a typical spectrum from a photoemulsion experiment on the ^{29}Si(^{3}He, d)^{30}P reaction at $\theta_{lab} = 23^\circ$. It is to be noted that the ordinate of Fig. 2 uses a "universal" scale where 0 to 10 counts are plotted on a linear scale and counts ≥ 10 are plotted on a log scale. This was done to reduce the background emphasis characteristic of a pure log scale, yet retain the range of amplitudes that may be shown on a single graph. Excitation energies $E_x \leq 7.1$ MeV were determined to an accuracy of ≅ ± 5 keV by using accurately known values of E_x (Refs. 12, 14, and 15) and by interpolating and extrapolating a smooth correction curve to a coarse magnet calibration. This correction is not included in the horizontal scales of Fig. 1 and varied from about − 5 keV at 1 MeV excitation energy to about − 30 keV at 7 MeV. The self-consistent set of excitation energies arrived at is given in Table I for the ^{29}P states and in Tables II and III along with energies[12] previously measured for the ^{30}P states. The procedure to fit standard peak shapes to the experimental spectra with the code AUTOFIT works well for ^{30}P states up to about 7 MeV. Above 7 MeV a few unresolved groups of states were decomposed by this method. The cross sections derived this way are thus quite uncertain for the decomposed groups of states at 7.2, 7.3, and 7.8 MeV. For example, the group near 7.3 MeV may be essentially a single state of large (20–30 keV) natural width.

For most angles the different kinematics allowed ^{30}P peaks to be distinguished from ^{29}P peaks which resulted from the 7.7% of ^{28}Si in the enriched ^{29}Si target. At a few angles ^{29}P contaminant peaks

TABLE II. Spectroscopic strengths $G_j=(2J_f+1)(2J_i+1)^{-1}C^2S_j$ for proton stripping to ^{30}P states below 7.1 MeV.

E_x [a] (keV)	E_x [b] (keV)	$J^\pi; T$ [a,b]	nlj	G_j (^{3}He, d) [b] at 25 MeV	G_j (^{3}He, d) [c] at 15 MeV	G_j (d, n) [d] at 8 MeV	Shell [e] model
0.0	0.0	1^+	$2s_{1/2}$	0.74	0.72	0.71	0.92
677.2 ± 0.4	677	$0^+;1$	$2s_{1/2}$	0.23	0.25	0.23	0.31
709.01 ± 0.15	709		mixed $2s_{1/2}$	0.09	0.09		0.01
			$1d_{3/2}$	0.45	0.35	0.6	0.57
1454.0 ± 0.5	1454	2^+	$1d_{3/2}$	<u>0.81</u>	0.81	0.84	0.80
			or $1d_{5/2}$	(0.61)	···	···	0.08
1973.0 ± 0.9	1973	3^+	mixed $1d_{5/2}$	0.12	0.07	0.21	0.26
			$1g_{7/2}$	0.21	···	···	···
2538.0 ± 0.7	2538	3^+	mixed $1d_{5/2}$	0.09	0.11	0.18	0.04
			$1g_{7/2}$	0.23	···	···	···
2723.2 ± 0.5	2723	2^+	$1d_{3/2}$	<u>0.10</u>	0.10	0.15	0.13
			or $1d_{5/2}$	(0.08)	···	···	0.03
2838.8 ± 1.0	2838	1^+	$1d_{3/2}$	0.04	···	···	0.01
			$2s_{1/2}$	~0	···	···	0.00
2937.8 ± 0.9	2939	$2^+;1$	$1d_{3/2}$	<u>0.80</u>	0.83	0.70	0.73
			or $1d_{5/2}$	(0.60)	···	···	0.08
3018.6 ± 0.9	3018	1^+	mixed $2s_{1/2}$	0.08	0.12	0.10	0.00
			$1d_{3/2}$	0.11	0.05	0.068	0.05
···	3304	(1^+)*	if $2s_{1/2}$	0.01	···	···	···
3731 ± 3	3731	1^+*	mixed $2s_{1/2}$	0.03	0.06	0.03	···
			$1d_{3/2}$	0.08	0.02	0.11	···
3834.3 ± 1.3	3834	$(1, 2^+), (3^+)$*	mixed $1d_{5/2}$	0.11	0.14	0.19(2^+)	0.05 (if 3^+)
			$1g_{7/2}$	0.11	···	···	···
3927.3 ± 1.3	3927	1^-	$2p_{3/2}$	0.005	(0.12) [f]		
			(if $2s_{1/2}$	0.01)	···		
4143.6 ± 1.1	4142	2^-	mixed $2p_{3/2}$	0.14	0.26	0.13	0.15
			($1f_{5/2}$	0.11)	···	···	···
4182.7 ± 1.3	4182	$2^+;1$	$1d_{3/2}$	<u>0.20</u>	0.15	···	0.13
			or $1d_{5/2}$	(0.16)	···	···	0.01
4230.2 ± 1.1	4232	4^-	$1f_{7/2}$	1.10	1.35	0.97	···
4234.5 ± 1.8							
4298 ± 5	4298		(if $2s_{1/2}$	0.005)			
4342.8 ± 1.0	4343			g			
4425 ± 3	4423	2^+	$1d_{3/2}$	<u>0.01</u>	(0.13) [f]	···	0.01
			or $1d_{5/2}$	0.01			0.01
			(if $2p_{3/2}$	0.01)	···	···	···
4468 ± 3	4468	$0^+;1$	$2s_{1/2}$	0.11	0.19	0.058	0.005 [h]
4501 ± 3	4501	$1^+;1$	$1d_{3/2}$	0.47	0.40	0.32	0.53
			$2s_{1/2}$	~0	···	···	0.00
4624.6 ± 1.2	4625	3^-	$1f_{5/2}$	(0.80)	···	···	
			or $1f_{7/2}$	<u>0.54</u>	0.65	0.56	1.26
4734 ± 10	4739	$(1^+, 2^+, 3^+)$*	$1d_{3/2}$	0.01	···	···	
4921 ± 3	4933	3^-	$1f_{7/2}$	···	0.04	0.28	
		or $(0, 1, 2)^-$*	$2p_{3/2}$	0.02	···	···	
5024 ± 10	5028		(if $2p_{3/2}$	0.002)	···	···	
5233 ± 10	5233	$(2, 3, 4)^-$*	$1f_{7/2}$	0.01	···	···	
5412 ± 10	5416	$(0, 1, 2)^-$	$2p_{3/2}$	0.07	(0.45) [f]	0.063	0.08
5504 ± 10	5505	1^+*	mixed $2s_{1/2}$	0.03	···	···	
			$1d_{3/2}$	0.05	0.08	0.19 [i]	
5598 ± 10	5574	$(2^+, 3^+; 1)$*	mixed $1d_{5/2}$	0.07	0.11	···	
			$1g_{7/2}$	0.09	···	···	
5700 ± 10	5711	···		weak			
5790 ± 10	5808	$(1^+, 2^+, 3^+; 1)$* [d]	(if $1d_{5/2}$	0.03)	···	···	
5916	5905	$(1, 2)^-$	$2p_{3/2}$	0.35	0.50	($l=1$)	
6002	5993	1^-d	$2p_{3/2}$	0.33	0.29	($l=1$)	
···	6092	$3^-;1$*	$1f_{5/2}$	0.90	···	($l=2$)	
			or $1f_{7/2}$	<u>0.59</u>			

TABLE II *(Continued)*

E_x [a] (keV)	E_x [b] (keV)	$J^\pi; T$ [a,b]	nlj	G_j (^{3}He, d) [b] at 25 MeV	G_j (^{3}He, d) [c] at 15 MeV	G_j (d, n) [d] at 8 MeV	Shell [e] model
···	6179	···		g			
···	6231	···	(if $2s_{1/2}$	0.03)			
6275	6270	2^-	$2p_{3/2}$	0.06			
6307	6301	3^+		j			
6486	6478	$1(+)^*$	$2s_{1/2}$	0.05			
6526	6518	$(1,2,3)^{+*}$	$1d_{3/2}$	0.04			
···	6599	···	(if $2s_{1/2}$	0.05)			
			(if $1d_{3/2}$	0.03)			
···	6648	$(2^-, 3^-, 4^-)^*$	($1f_{5/2}$	0.05)			
			(or $1f_{7/2}$	0.04)			
6684	6674	···	(if $2p_{3/2}$	0.02)			
			(if $2s_{1/2}$	0.04)			
···	6789	···	(if $2s_{1/2}$	0.04)			
6859	6851	1	(if $1d_{3/2}$	0.05)			
			(if $2p_{3/2}$	0.03)			
6883	6877	2^-	$2p_{3/2}$	0.34	···	($l=1$)	
6927	6921	1^-	$2p_{3/2}$	0.23	···	($l=1$)	
7023	7013	2^-	$2p_{3/2}$	0.05	···	($l=1$)	
7056	7048	$4^-; 1^*$	$1f_{7/2}$	0.95	···	($l=2$)	1.62

[a] Reference 12.
[b] This work. New spin, parity, and isospin assignments are indicated by an asterisk. Errors in excitation energies are ±5 keV.
[c] Reference 21.
[d] Reference 22.
[e] Reference 23 for positive parity states, Ref. 22 for negative parity states.
[f] Order of magnitude discrepancies in Ref. 21 are apparently due to typing errors.
[g] Structureless angular distribution. $d\sigma/d\omega \leq 0.05$ mb/sr.
[h] The theoretical prediction (Ref. 23) for the third 0^+, $T=1$ state is $G=0.04$.
[i] A pure $l=2$ is assumed in Ref. 22.
[j] Incomplete angular distribution because of contaminations.

superimposed on ^{30}P groups were subtracted out using the data on the enriched ^{28}Si target.

C. Measurements at 0°

In transfer reactions on odd-A the nuclear states may be excited through a mixture of orbital angular momentum transfer. The resulting angular distributions are the sums of those that result from single l transfers. Analysis of these components into constituent angular distributions can be facilitated considerably by finding the cross section at 0° scattering angle if one of the components is $l=0$, because in this case the cross section rises sharply at far forward angles. This forward angle rise distinguishes an $l=0$ component clearly from an $l=2$ component. To take spectra at 0° scattering angle the Faraday cup which is situated in the scattering chamber was moved out of the way automatically as the spectrometer was rotated to angles smaller than 6°. The primary beam would then pass into the spectrometer. This beam was caught in another Faraday cup which could be moved along the focal surface of the spectrometer to accommodate a range of magnetic field settings. The spectrometer entrance aperture width was set to 0.5°. Both a position solid state detector and photoemulsions were used for the 0° measurements. The detector was protected from neutrons produced in the Faraday cup with lead shielding, and foils covered both the detector and the photoemulsions to eliminate tritons, ^{3}He, and α particles.

D. Elastic ^{3}He scattering on ^{28,29,30}Si

The elastic scattering data were taken with solid state position-sensitive detectors in the spectrometer for about 30 angles for each of the three stable Si isotopes. At forward angles the enriched targets were used. For $\theta \gtrsim 30°$, where the three ^{3}He groups scattered off each of the isotopes are resolved, the "mixed" target of approximately equal quantities of each Si iso-

TABLE III. Spectroscopic strength $G_j = (2J_f+1) \times (J_i+1)^{-1} C^2 S_j$ for ^{29}Si(^{3}He, d) at 25 MeV to ^{30}P states above 7.1 MeV. (A continuation of Table II. No previous proton transfer data are available for $E_x > 7.1$ MeV.)

E_x [a] (keV)	E_x [b] (keV)	$J^\pi; T$ [a,b]	nlj	G_j
7186	7176	1^-	$2p_{3/2}$	0.17
7206	7199	···	if $1d_{3/2}$	0.18
			if $2p_{3/2}$	0.12
7230	7224	2^-	$2p_{3/2}$	0.15
7288	7281	3	(if $1d_{3/2}$	0.06)
7291		2^+	(if $2p_{3/2}$	0.05)
7314	7308	$(3), (2,3,4)^{-*}$	$1f_{5/2}$	0.30
7316			or $1f_{7/2}$	0.21
7331	7328	1^-	$2p_{3/2}$	0.12
7391	7380	···	(if $2p_{3/2}$	0.05)
···	7472	···	if $1d_{3/2}$	0.33
			if $2p_{3/2}$	0.22
7503	···	1^+	···	···
7572	7559	$(1,2,3)^+$	$1d_{3/2}$	0.04
7591	7582	$(2,3,4)^-, (2^-)^*$	$2p_{3/2}$	0.21
7615	7606	3^+	···	c
7654	7643	$(1,2,3)^+$	···	c
···	7690	···	(if $2p_{3/2}$	0.05)
7755	7751	1^-	(if $2p_{3/2}$	0.06)
7760		0^+	(if $2s_{1/2}$	0.10)
			(if $1d_{3/2}$	0.09)
7888	7897	2^-	$2p_{3/2}$	0.10
7932		$(1,2,3)^+$	or $1d_{3/2}$	0.16
···	8109	···	(if $1f_{7/2}$	0.07)
···	8202	···	(if $2p_{3/2}$	0.05)
···	8282	···	(if $2p_{3/2}$	0.06)
···	8353	···	(if $2p_{3/2}$	0.06)
			(if $1d_{3/2}$	0.09)
···	8628	$(2^-, 3^-, 4^-)^*$	$1f_{5/2}$	0.30
			or $1f_{7/2}$	0.22

[a] Reference 12.

[b] This experiment. New spin, parity assignment indicated by an asterisk. Errors in excitation energies are ±10 keV.

[c] Incomplete angular distributions because of contaminations.

tope was used. This allowed all three angular distributions to be taken simultaneously. Figure 3 shows the experimental data together with the optical model fit (see below). An over-all normalization of the cross sections to an accuracy of about 15% was obtained from the minimum in the χ^2 of the optical model fit as a function of the normalization constant.

III. ANALYSIS OF DATA

A. Optical model analysis

The optical model fit to the elastic scattering data was optimized using the computer code RAROMP.[16] Potentials of standard Wood-Saxon geometry with volume absorption were used. A spin-orbit term was not included. Several different starting potential parameters ($V_r \cong 80$, 140, 180 MeV) which we tried yielded fits of very similar quality. The optical model fits with the $V_r = 140$ MeV set (Table IV), which gave the best fit to the transfer data, are shown in Fig. 3 for the three stable Si isotopes.

B. DWBA–Analysis of the ^{28,29}Si(^{3}He, d)^{29,30}P reactions

Distorted-wave Born approximation (DWBA) calculations have been performed using the computer code DWUCK.[10] Finite range and nonlocality corrections were not included. Bound state parameters are given in Table IV. First calculations were performed using the three different ^{3}He optical model parameter sets which we

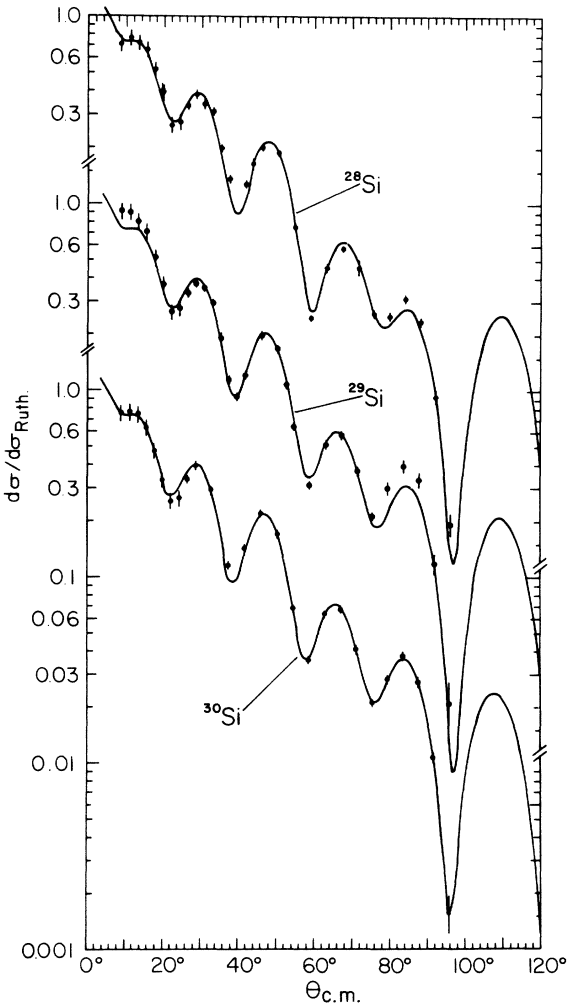

FIG. 3. Angular distributions from elastic scattering of ^{3}He at 25 MeV on the three Si isotopes. Solid lines are the optical model fits.

TABLE IV. Optical model parameters used in DWBA calculations.

Set	Channel	E_{lab} (MeV)	V_r (MeV)	r_r (fm)	a_r (fm)	W_v (MeV)	$4W_D$ (MeV)	r_i (fm)	a_i (fm)	V_{so} (MeV)	r_c (fm)
A [a]	^{28}Si + d	34.4	94.3	1.046	0.807	...	44.0	1.357	0.733	7.0	1.3
B [b]	^{28}Si + ^{3}He	25.0	148.7	1.098	0.762	15.32	...	1.755	0.754	...	1.4
C [b]	^{29}Si + ^{3}He	25.0	142.0	1.101	0.762	16.46	...	1.723	0.755	...	1.4
D [b]	^{30}Si + ^{3}He	25.0	140.5	1.101	0.768	16.17	...	1.742	0.728	...	1.4
E	^{28,29}Si + p	...	Adjusted	1.25	0.65	...	...	...	...	(λ = 25) [c]	1.25

[a] Reference 17.
[b] This work.
[c] Spin-orbit potential of 25 times the Thomas-Fermi term.

derived from a fit to the elastic scattering on ^{29}Si. These three ^{3}He parameter sets are drawn into Fig. 4. A single deuteron optical model set[17] (Table IV) was used to study the effect of the different ^{3}He potentials on $l = 0$ and $l = 2$ transitions. Clearly, the $V_r = 142$ MeV set gives the best fit to the (^{3}He, d) proton transfer data (Fig. 4). Therefore, we used the 140 MeV sets which are listed in Table IV for the final DWBA calculations to extract spectroscopic factors. The results of the DWBA calculations are shown together with the experimental angular distributions in Fig. 5 for ^{28}Si(^{3}He, d) and in Figs. 6–8 for the ^{29}Si(^{3}He, d). The latter three figures were drawn in part with the aid of the computer code AUTOFIT.[13] The angular distributions are labeled by the n, l, j values which we assumed for the orbit to which the particle is transferred.

The proton becomes unbound in ^{29}P at $E_x = 2744$ keV, i.e., only the ground state and first three excited states are bound. In ^{30}P, states above 5600 keV are proton unbound. For these states a special adaption to DWUCK was used.[10] This code uses the outgoing Coulomb wave function for points at $r \geq R_{max}$ instead of the usual zero boundary condition for the wave function at R_{max}. Satisfactory fits were obtained for a number of unbound levels. However, for highly excited states (≥ 7 MeV) the modified DWBA produced very oscillatory curves, especially for $2s_{1/2}$ and $1p_{3/2}$ transfer, which do not fit the data as well as the shapes calculated for lower excita-

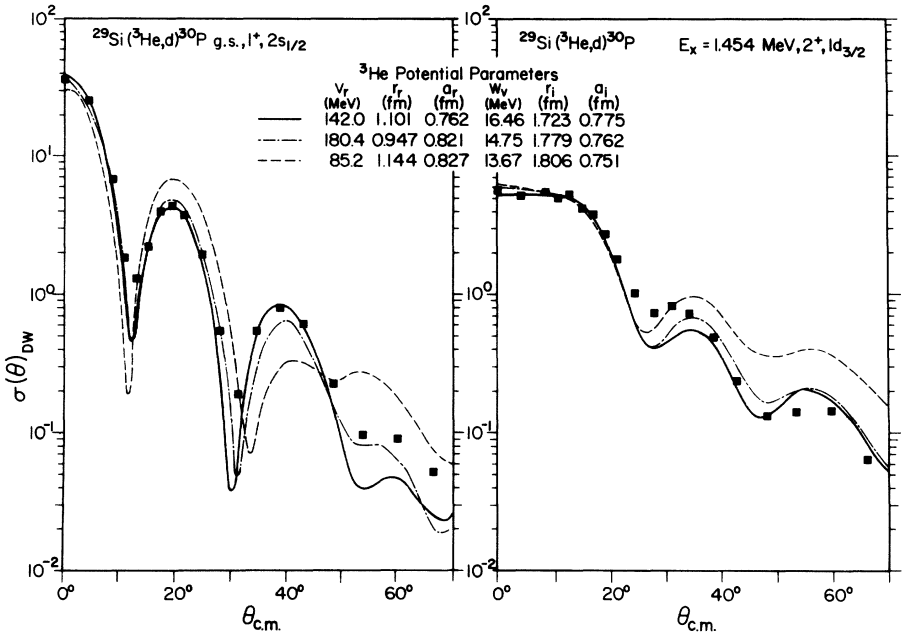

FIG. 4. DWBA predictions for $2s_{1/2}$ and $1d_{3/2}$ transitions to two states in ^{30}P using three different sets of ^{3}He potentials. The vertical scale is for $\sigma_{DW}(\theta)$. Experimental data points $\sigma_{exp}(\theta)$ are multiplied by $(2j+1)/G_j N$ (see Sec. IV) in this figure only.

tion energies. We have therefore used the $2p_{3/2}$ curve calculated for the ^{30}P (6674 keV) state for all $l=1$ candidates above that energy. We also used the ^{29}P(g.s.) $2s_{1/2}$ calculation to fit the ^{29}P (4754 keV) state angular distribution. Furthermore, the search for the proton potential did not converge for the $1g_{7/2}$ (and $1g_{9/2}$) transitions above 4.5 MeV in ^{29}P. Therefore, the 4075 keV $1g_{7/2}$ curve was used for the 6317 keV state. We tentatively assign $J^\pi = \frac{9}{2}^+$ to this latter state because it is probably the analog of the $\frac{9}{2}^+$ state seen at 6779 keV in the ^{28}Si$(d,p)^{29}$Si reaction.[8,9]

^{30}P states populated by mixed l transfer (most importantly, mixed $l=0$ and $l=2$) were decomposed with the aid of the computer code CURVEFIT.[18] In general the fits to the low lying states are excellent. The shapes of the angular distribution for the 3^+ states at 1973 and 2538 keV show a shape distinctly different from that for the $l=2$ ($1d_{3/2}$ or $1d_{5/2}$) transition to the 2^+ states. The 3^+ may be reached either by $1d_{5/2}$ or $1g_{7/2}$ transfer. In fact, very good fits are easily obtained by a mixture of $1d_{5/2}$ and $1g_{7/2}$ curves. However, the shape difference may be the result of a j dependence[19] or of two-step processes which can be very important for weakly excited states. The extracted $l=4$ strength should be taken merely as indicative of the shortcomings of the standard

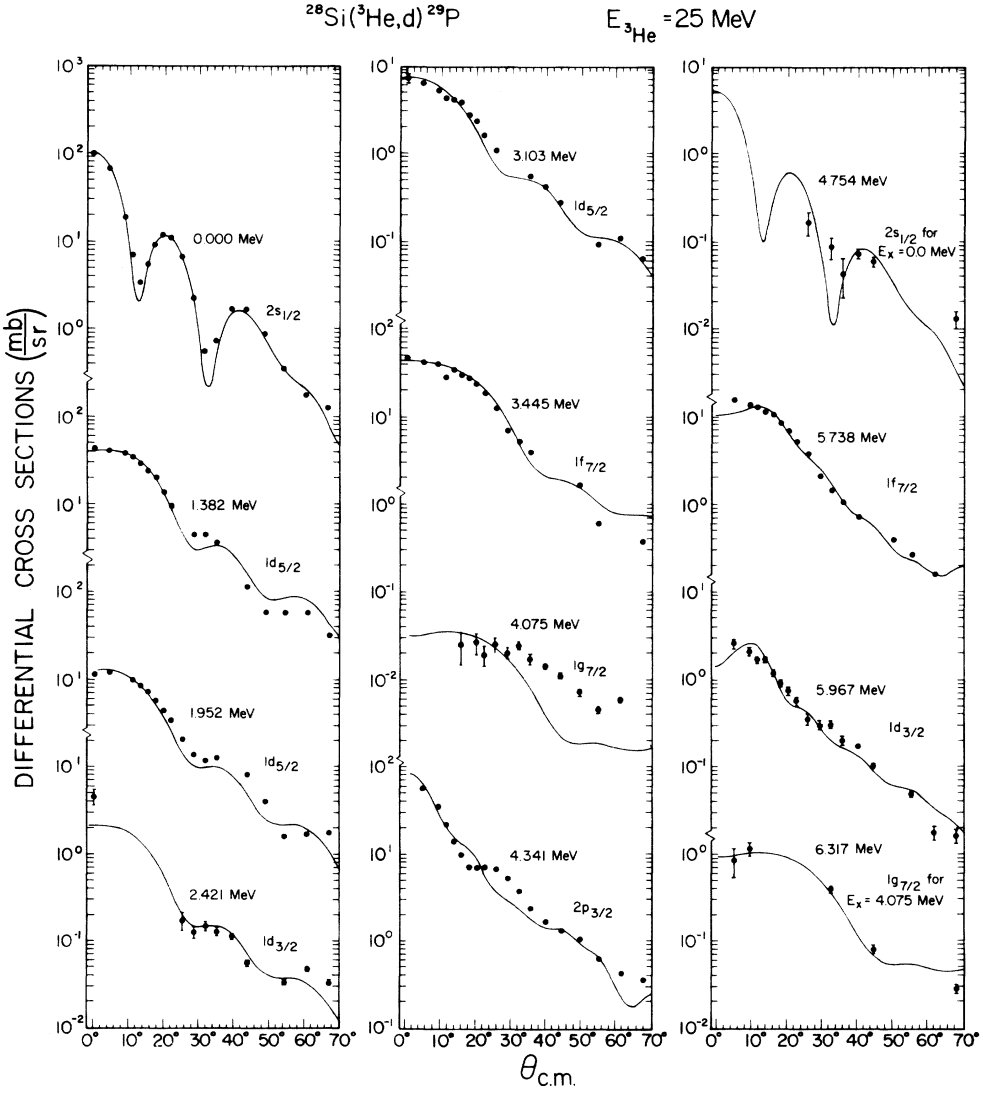

FIG. 5. Angular distributions and distorted-wave curves for the ^{28}Si(^{3}He, d)^{29}P reaction. Errors shown are due to statistics and background subtraction only. They do not include the over-all uncertainty of 15% in the absolute cross section.

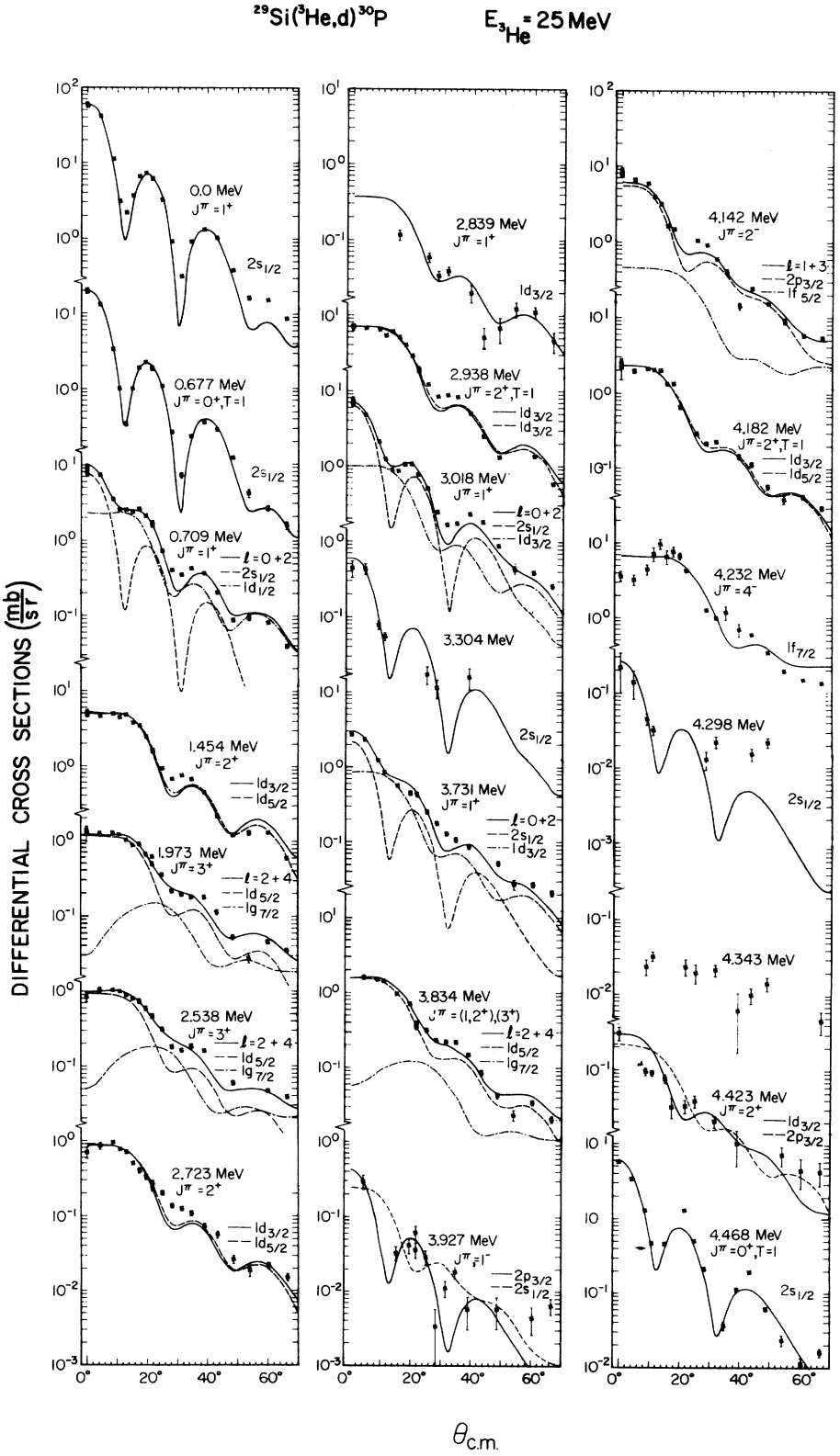

FIG. 6. Angular distributions and distorted-wave curves for the ^{29}P(^{3}He, d)^{30}P reaction.

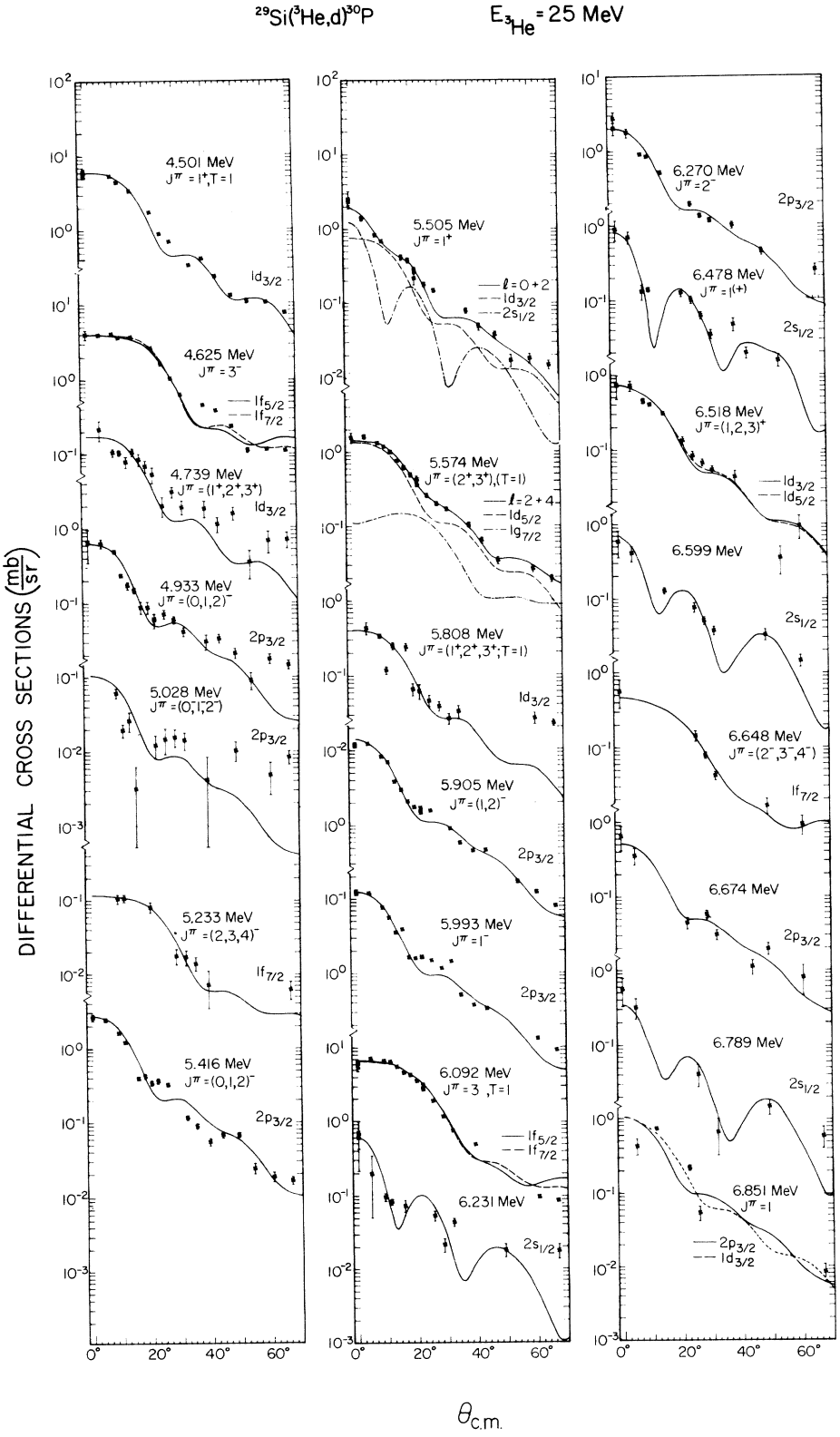

FIG. 7. Continuation of Fig. 6.

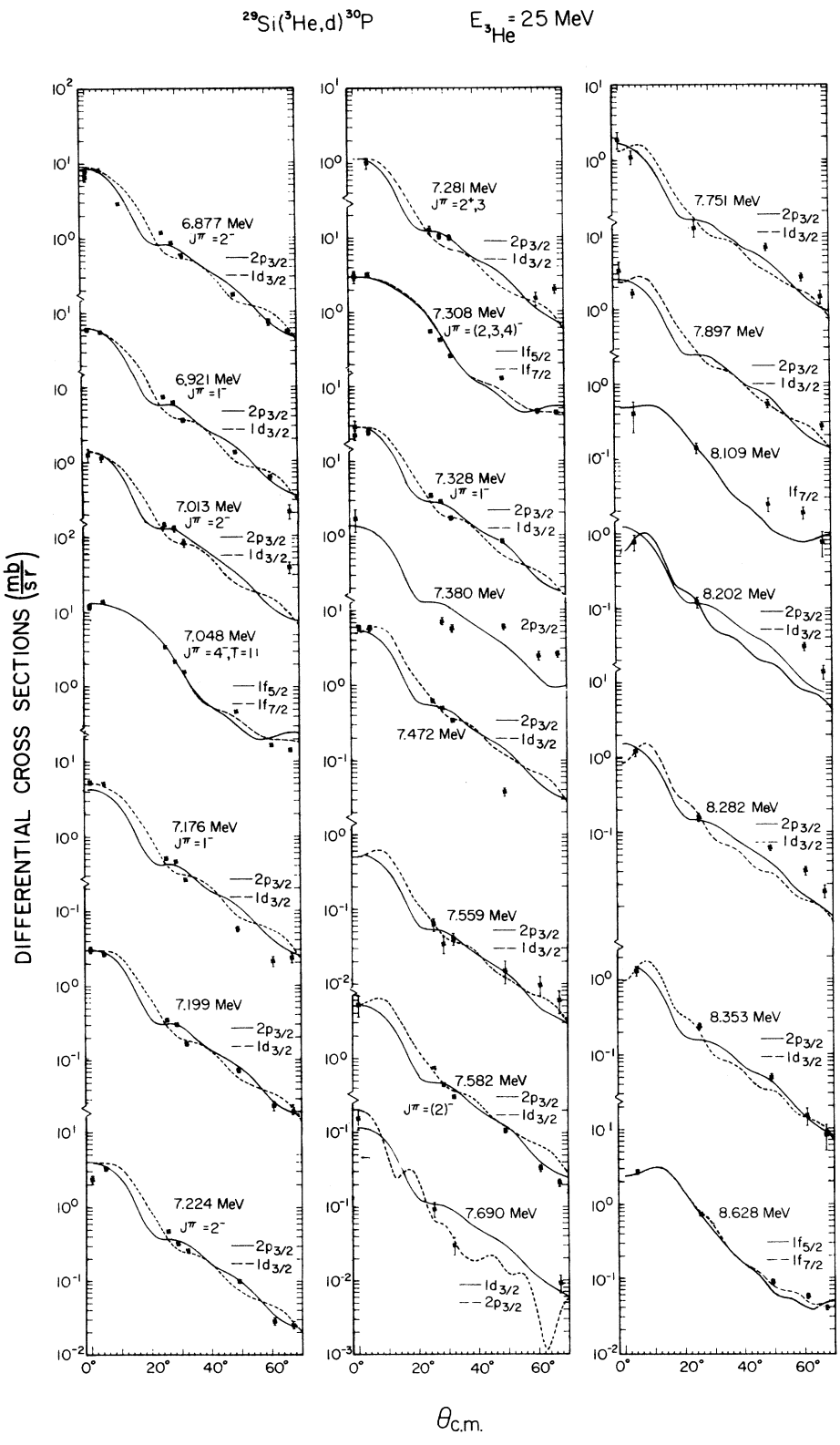

FIG. 8. Continuation of Fig. 7.

single-step DWBA. They do not decrease the extracted $1d_{5/2}$ strengths by more than 5–10% because the calculated $l=4$ cross sections are very small at the forward maxima of the $l=2$. The shape of the $l=2$ angular distribution to the 3834 keV state is similar to those for the known 3^+ states. We therefore tentatively assign $J^\pi = 3^+$ to this state.

IV. RESULTS

A. Spectroscopic strengths for ^{28}Si(^{3}He, d)^{29}P

Absolute spectroscopic strengths $G_j = [(2J_f+1)/(2J_i+1)]C^2S_j$ were extracted by normalizing the experimental angular distributions $\sigma_{exp}(\theta)$ to the DWBA calculations $\sigma_{DW}(\theta)$. J_i and J_f are the spins of the target and residual nuclei, respectively. $C^2=1$ for ^{28}Si(^{3}He, d)^{29}P and $C^2=\frac{1}{2}$ for ^{29}Si(^{3}He, d)^{30}P. S_j are the spectroscopic factors. Bassel's[20] normalization constant $N=4.43$ was used to derive the values of

$$G_j = \frac{2j+1}{N}\frac{\sigma_{exp}(\theta)}{\sigma_{DW}(\theta)} ,$$

where j is the total angular momentum of the transferred particle. The results for the proton transfer to ^{29}P states are given in Table I. The factor of 2 discrepancy between the G_j values of this work and Ref. 7 for a number of states may be due to the extrapolation procedure used[7] to extract spectroscopic factors for transitions to unbound levels. Also given are the strengths derived from ^{28}Si(d, p)^{29}Si reactions.[8,9] The reasonable agreement between the ^{28}Si(^{3}He, d)^{29}P strength to the proton unbound levels, e.g., the $\frac{3}{2}^-$ state at 4341 keV and the ^{28}Si(d, p) strength for the neutron bound $\frac{3}{2}^-$ state in the mirror nucleus ^{29}Si (4934 keV), indicates the usefulness of the modified[10] DWBA to calculate transitions to unbound states. It should be noted that both (^{3}He, d) and (d, p) to the $\frac{7}{2}^-$ mirror states at 3445 and 3624 keV appear to contain only about one-half of the total $1f_{7/2}$ strength of 8.

B. Spectroscopic strengths for ^{29}Si(^{3}He, d)^{30}P

The spectroscopic strengths for the ^{29}Si(^{3}He, d)^{30}P reaction are given in Tables II and III. Here, for mixed transitions of the same l, differing only in transferred j, the strengths are given for both possible j values. These $l=2$ (or $l=3$) strengths are not the result of a superposition of $1d_{3/2}$ and $1d_{5/2}$ (or $1f_{5/2}$ and $1f_{7/2}$) DWBA curves which differ only very little in shape. Whenever these two values are given, the one expected to be the principal component in the transition is underlined and used later in the application of the sum rules. In contrast, the mixed $l=0$, $l=2$ transition to 1^+ states has been fitted by a superposition of theoretical curves and thus the two spectroscopic strengths are those of the contributing $2s_{1/2}$ and $1d_{3/2}$ components. It is worth mentioning that the only observed $J^\pi = 1^+$, $T=1$ state at 4.5 MeV appears to be excited by a pure $l=2$ transition while the many $J^\pi = 1^+$, $T=0$ states are excited by mixed $l=0$, $l=2$ transitions.

Also shown in Table II are G_j values from previous (^{3}He, d) [21] and (d, n) [22] experiments and from theoretical predictions.[23] In general, good agreement between the various experiments is found with a number of notable exceptions. A number of weak transitions, in particular $1d_{5/2}$ hole transitions, vary by factors of 2 to 3 for the three experiments. This could be due to two-step excitations in weak transitions which have a different energy and projectile dependence. In a few cases there appear to be typographical errors in the absolute strengths of Ref. 21. There, G_j values for the 3927, 4423, and 5416 keV states are given which are an order of magnitude larger than our values or than indicated by the differential cross sections of Ref. 21. We agree in all l assignments for the transitions to states up to 4625 keV. We assign tentatively $J^\pi = (1^+, 2^+, 3^+)$ to the 4739 keV state based on an $l=2$ shape.

A state at 4921 keV was given[21] a $J^\pi = 3^-$ assignment based on an $l=3$ shape of the angular distribution. Our differential cross sections for this state which we locate at 4933 keV show a good $l=1$ shape. Thus, we assign $J^\pi = (0, 1, 2)^-$. That the wrong l value was assumed in the (^{3}He, d) [21] and also in the (d, n) experiment[22] is also indicated by the factor of 7 discrepancy between the (^{3}He, d) and (d, n) reactions when an $l=3$ is fitted to the data. There are no such discrepancies between (^{3}He, d) and (d, n) for well established $l=3$ transitions. $J^\pi = (2, 3, 4)^-$ may be assigned to the 5233 keV state, also based on the shape of the angular distribution. For the 5505 keV state we find a mixed $l=0$, $l=2$ angular distribution from which we derive $J^\pi = 1^+$, ($T=0$). The $l=0$ component was not seen before.[21,22] Our $T=0$ assignment is based on the fact that there is no $J^\pi = 1^+$ state known in ^{30}Si at the corresponding energy. We reject the tentative $J^\pi = (2^+, 3^+)$, $T=1$ assignment[21,22] for this state.

To facilitate a comparison of ^{30}Si states with $T=1$ states in ^{30}P, excitation energies are shown in Fig. 9 together with spectroscopic strengths G_j for the reactions of interest: ^{29}Si(^{3}He, d)^{30}P and ^{29}Si(d, p)^{30}Si.[6] Also included are the results of the (^{3}He, d) and (d, p) reactions[8] on ^{28}Si for later use. We see all the known $T=1$ states in ^{30}P up to 4.5 MeV. We consider the peak at 5574

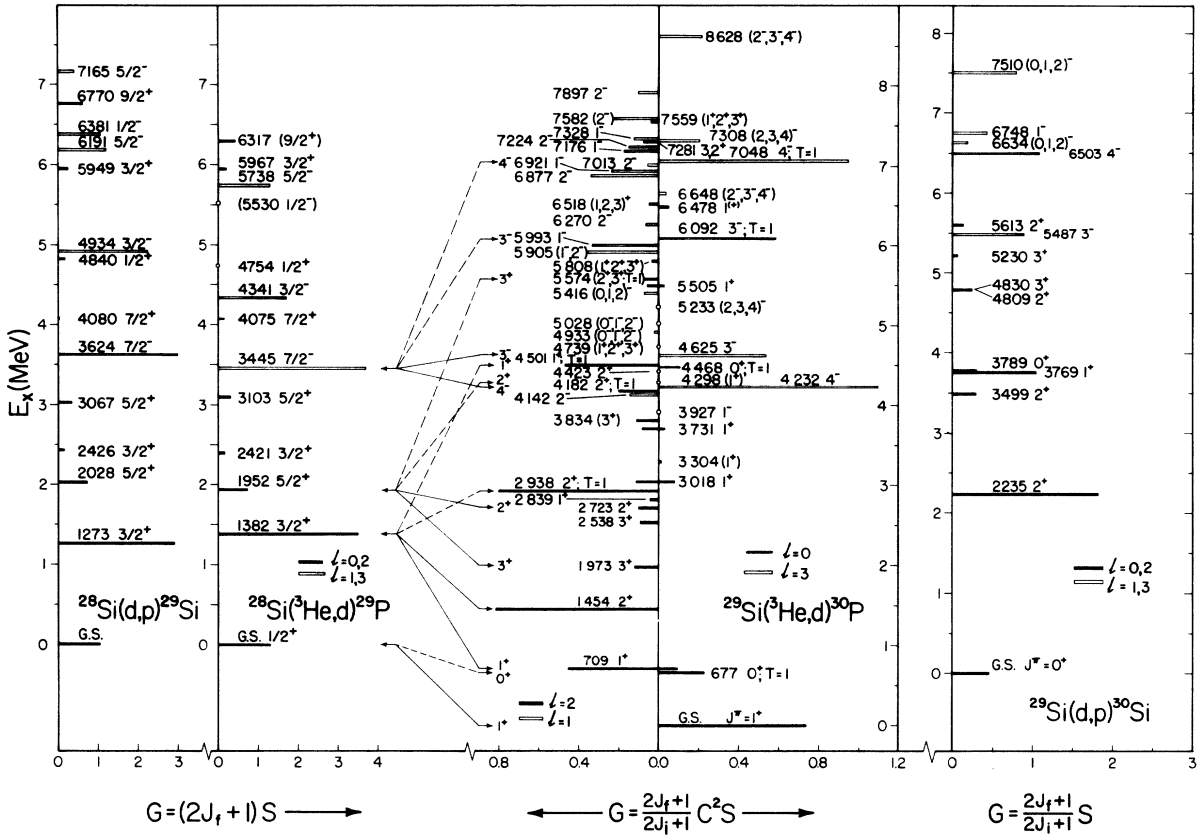

FIG. 9. Energy levels of ^{29}Si, ^{29}P, ^{30}P, and ^{30}Si and spectroscopic strengths for single-particle stripping reactions. Solid bars indicate the strengths of positive parity transitions, open bars—those to negative parity states. For ^{29}Si-(^{3}He, d)^{30}P the $l=1$ and $l=2$ transitions are drawn to the left, the $l=0$ and $l=3$ transitions to the right. The thin lines between mass 29 and mass 30 energy levels indicate possible relations between single-particle states in mass 29 and two-particle states in mass 30. Solid lines: $T=0$, broken lines: $T=1$.

keV a candidate for the analog of one or both states of the $2^+, 3^+$ doublet at 4.8 MeV in ^{30}Si. The 5230 keV, 3^+ state in ^{30}Si may have its analog at 5808 in ^{30}P to which we assign $J^\pi=(1^+, 2^+, 3^+;\ T=1)$. The 5230 keV state of ^{30}Si is very strongly excited[24] in ^{31}P(d, ^{3}He) indicating a principal $(1d_{5/2})^{-1}(2s_{1/2})^3$ component. A transition of similar strength in ^{31}P(d, t) or (p, d) would identify the analog 3^+, $T=1$ state in ^{30}P unambiguously.

Rather clear are the analog relationships between the 3^- and 4^- states in ^{30}Si at 5487 and 6503 keV, respectively, and the 6092 and 7048 keV states in ^{30}P. Both of these states are excited by very strong $l=3$ transitions. Thus, these states carry the bulk of the $(1f_{7/2}2s_{1/2})_{3^-,4^-;T=1}$ strength. We assign $J^\pi=3^-$, $T=1$ to the 6092 keV state and $J^\pi=4^-$, $T=1$ to the 7048 keV state, because the 4^-, $T=1$ state of the $(2s_{1/2})(1f_{7/2})$ configuration is expected[25] to lie above the 3^-, $T=1$ state in contrast to the 4^-, $T=0$ state which is expected and observed below the 3^-, $T=0$ state. This 4^- assignment supports the spin given by Ref. 26.

Reference 22 assigned $l=2$ to the transitions to both of these states based on the shape of the (d, n) angular distributions. It is likely that the procedure they used for the DWBA calculations for the unbound states does not predict the shapes of the (d, n) angular distributions correctly.

For the other states above 5 MeV it is very difficult to deduce information on analog relations because of the high density of states. However, the strong $l=1$ transitions seen in (d, p) appear to be matched by a number of $l=1$ transitions seen in (^{3}He, d).

New spin assignments for other states are tentative (see Tables II and III) and based mostly on shapes of angular distributions. Unfortunately, $l=1$ and $l=2$ shapes are not sufficiently different for the states above 6 MeV excitation. For this reason, two G_j values (for $2p_{3/2}$ and $1d_{3/2}$ transfer) are frequently given unless the parity of the state was known from previous experiments.

C. Sum rules

In the following paragraphs we will frequently make use of the well known sum rule[27]: The number of proton holes in the shell model orbit of quantum numbers n, l, j, is given by $\sum G_j$ where the sum is to be extended over all states which are reached by transfer of a certain n, l, j. For stripping to empty orbits of angular momentum j we have $S_j = 1$ for each of m states of spin $\vec{J}_f = \vec{j} + \vec{J}_i$ (where J_i is the target spin, $\frac{1}{2}$ in our case) so that the total strength G_j is divided between the m states simply according to their statistical weights $(2J_f^{(m)}+1)/\sum_m(2J_f^{(m)}+1)$. These weights also apply for partially filled orbits if the transferred nucleon is weakly coupled to the target ground state. In practice, the partial strengths for each of—in our case—two states of $J_f^{(1)} = j + \frac{1}{2}$ and $J_f^{(2)} = j - \frac{1}{2}$ will be shared by a number k of states for which we expect the following sum rules to hold under either of the above mentioned conditions:

$$\sum_k G_j(k) = (\text{number of proton holes})_j \frac{2J_f^{(m)}+1}{\sum_n 2J_f^{(m)}+1} .$$

In the sums for individual orbits we will include only those transitions for which the j transfer is reasonably well known. Not included will be all those G_j values of Tables II and III which have an "if" placed in front of the n, l, j values. Whenever an "or" is placed in front of one of the n, l, j values, the one underlined will be used.

D. $(2s_{1/2})(1f_{7/2})_{3^-,4^-}$ configuration

As noted above, the $J^\pi = 3^-$ and 4^-, $T = 1$ states were identified by the $l = 3$ shape of the angular distribution, their large strength in the ^{29}Si(^{3}He,d)^{30}P reaction, and their energies. They were not seen in the ^{31}P(d, ^{3}He)^{30}P reaction[24] which supports the assignment of a $(2s_{1/2})(1f_{7/2})$ configuration for these states. The $l = 3$ strengths which we derive for these transitions are in fact very close to those for the well known 4232 keV (4^-, $T = 0$) and 4625 keV (3^-, $T = 0$) states. Apparently, these latter states are the antianalog states of the just mentioned $3^-, 4^-$; $T = 1$ states.

The shell model limit for the transition strength to the $(2s_{1/2})(1f_{7/2})_{3^-,4^-}$ configuration is $\sum G_j = 8$, half of which should be found in transitions to $T = 0$, the other half in transitions to $T = 1$ states. For each isospin the strength would be divided between the J_f, $J_f' = 3^-, 4^-$ pair of states according to a ratio $\frac{7}{9}$. Thus, we expect $G_j = 1.75$ for the transitions to each of the $(2s_{1/2})(1f_{7/2})_{3^-}$ states ($T = 0$ and $T = 1$) and $G_j = 2.25$ in the transitions to each of the 4^- states. Experimentally we find $G_j = 0.5$ and $G_j = 1.0$ for the 3^- and 4^- states, respectively (both for $T = 0$ and $T = 1$), i.e., somewhat less than half of the total strength for the 4^- state and only about $\frac{1}{3}$ for the 3^- state. Similarly, the ^{28}Si(d, p) and (^{3}He, d) reactions to the lowest $\frac{7}{2}^-$ state also showed only about one-half of the total $1f_{7/2}$ strength (Table I). This may be either due to an insufficiency of the DWBA or more than one-half of the total $1f_{7/2}$ strength is still to be found at higher excitation energies both in mass 29 and 30 nuclei. In any case, both $3^-, 4^-$ doublets appear to be quite nice examples of weak coupling doublet states, i.e., coupling of a $2s_{1/2}$ particle to the $\frac{7}{2}^-$ state of mass 29. This is indicated in Fig. 9 by the thin lines that connect the ^{29}P spectrum with that of ^{30}P. There are two other $l = 3$ transitions to the states at 7308 and 8353 keV of non-negligible strength (Table III). They could be 3^- states and account for the fact that the 3^- states at 4625 and 6092 keV have only $\frac{1}{3}$ of the strength compared to $\frac{1}{2}$ in the 4^- states in ^{30}P and the $\frac{7}{2}^-$ state in ^{29}P. However, they could also be states of the $(2s_{1/2})(1f_{5/2})_{2^-,3^-}$ configuration.

E. $(2s_{1/2})^2_{0^+,1^+}$ and $(2s_{1/2})(1d_{3/2})_{1^+,2^+}$ configurations

The surprising purity of the 3^- and 4^-, $T = 0$ and $T = 1$ states in terms of a weak coupling model is in marked contrast to the splitting of the $(2s_{1/2})^2$ and $(2s_{1/2})(1d_{3/2})$ strengths between a large number of 1^+, $T = 0$ states. We see six 1^+, $T = 0$ states of which four are excited by mixed $l = 0$ and $l = 2$ transitions, but only one 1^+, $T = 1$ state excited by a pure $l = 2$ transition. However, of the many 1^+, $T = 0$ states only the g.s. is very strongly excited by $2s_{1/2}$ transfer and the five other 1^+ states together have only $\frac{1}{3}$ of the g.s. strength. Similarly, the 1^+ state at 709 keV contains twice the $l = 2$ strength of all other 1^+ states together. That means even in the complex spectrum of 1^+, $T = 0$ states only one state each has a large fraction of the $(2s_{1/2})^2$ or the $(2s_{1/2})(1d_{3/2})$ strength. We observe a total of $\sum_{1^+} G_{3/2} = 0.73$ for all 1^+, $T = 0$ states close to the limit of $\frac{3}{4}$ for stripping to an empty $1d_{3/2}$ shell, but only 0.47 out of $\frac{3}{4}$ in the only 1^+, $T = 1$ state.

The combined $l = 0$ strength to all 1^+, $T = 0$ states is 0.97 out of a maximum $\sum_{1^+} G_{1/2} = \frac{3}{2}$ for all 1^+ states that could be reached by stripping into an empty $2s_{1/2}$ proton shell. The observed two 0^+, $T = 1$ states, with about $\frac{2}{3}$ of the combined strength in the 677 keV state exhaust 0.34 out of a maximum $\sum_{0^+} G_{1/2} = \frac{1}{2}$. The two 2^+, $T = 0$ and the two 2^+, $T = 1$ states show most of the strength in the lower lying of the two states and a summed strength each for $T = 0$ and $T = 1$ of about 1, which is close to the $(2s_{1/2})(1d_{3/2})_{2^+}$ limit value of $\frac{5}{4}$.

However, a small part of the transition strength to the 2^+ states would be due to a small $(1d_{5/2})^{-1}(2s_{1/2})^3$ admixture in the 2^+ states as discussed in the next section. Such a small $1d_{5/2}$ component in the presence of a strong $1d_{3/2}$ component has recently been determined for the 1454 keV state in ^{30}P from a comparison of light and heavy ion induced proton transfer reactions.[28]

In Fig. 9 we have again connected the ^{30}P states having strong two-particle components with the corresponding one-particle states in ^{29}P. Only the states with the strongest transitions to a certain shell model orbit were connected. In this context, it is interesting to note that a determination of centroids of excitation energies of states which have fractions of the two-particle state configurations gives very encouraging results[29] in comparison with effective interaction matrix elements.[25,30]

F. $(1d_{5/2})^{-1}(2s_{1/2})^3{}_{2^+,3^+}$ configuration

Excitation of 3^+ states in ^{29}Si(^{3}He, d)^{30}P by direct single-step proton transfer is evidence for a $(1d_{5/2})^{-1}(2s_{1/2})^3$ component in the ground state wave function of ^{29}Si, because the 3^+ states can be excited only by $1d_{5/2}$ transfer if we restrict our configuration space to the $2s1d$ shell. We see a number of weakly excited 3^+, $T=0$ states and a candidate for a 3^+, $T=1$ assignment at 5574 keV.

The $(1d_{5/2})^{-1}(2s_{1/2})^3{}_{2^+}$ configuration is expected to mix with the $(2s_{1/2})(1d_{3/2})_{2^+}$ configuration. Its strength may be estimated as $\frac{5}{7}$ of that to the 3^+ states. We have therefore subtracted $\frac{5}{7}$ of the transition strengths to the 3^+ states from that to the 2^+ states and included the result in the $\sum G_{5/2}$. We arrive at $\sum_{2^+,3^+} G_{5/2} = 0.7$ for the number of $1d_{5/2}$ proton holes in ^{29}Si.

G. $(2s_{1/2})(2p_{3/2})_{1^-,2^-}$ configurations

We observe a total of nine $l=1$ transitions with $G_j > 0.1$ to known negative parity states, indicating a considerable splitting of the $(2s_{1/2})(2p_{3/2})$ strength. The transitions to the 7199 and 7472 keV states also have G_j values larger than 0.1; however, the parities of these states are not known and the experimental angular distributions do not allow discrimination between $l=1$ and $l=2$ transfer. It is also possible that the unresolved group of states around 7.2 MeV is due to essentially two strong $l=1$ transitions to two broad states.

The lower lying 2^-, $(1,2)^-$, and 1^- states at 4142, 5905, and 5993 keV respectively are most likely $T=0$ states. The other strong $l=1$ transitions to states above 6.8 MeV probably go in part to $T=1$ states since a number of strong $l=1$ transitions are seen[6] in ^{29}Si(d,p) to ^{30}Si states of the corresponding energies. The negative parity spectrum is further complicated since at these energies the $(1p_{1/2})^{-1}(2s_{1/2})^3$, $(2s_{1/2})^1(2p_{1/2})^1$, etc., configurations are expected to mix with the $(2s_{1/2})(2p_{3/2})$ configuration.

H. Comparison with shell model predictions and total $2s1d$, $2p_{3/2}$, and $1f_{7/2}$ strengths

Spectroscopic strengths for positive parity states have been calculated[23] for proton stripping to ^{30}P states in a truncated $d_{5/2}$-$s_{1/2}$-$d_{3/2}$ basis space. The results are listed in Table II. In general there is good agreement between experimental values and theoretical predictions, in particular for the strongly excited states. However, there are a number of significant discrepancies in the $2s_{1/2}$ strength to the $J^\pi = 1^+$, $T=0$ states. This may be due to truncating the full $2s1d$ shell model space. Untruncated $2s1d$ shell model calculations have also been performed[31]; however, spectroscopic factors have not yet been calculated and the agreement with the experimental excitation energies is only fair. Not all experimentally observed 1^+ states were reproduced in these calculations. The 3834 keV which we tentatively assign $J^\pi = 3^+$ is perhaps the third 3^+ level predicted[31] at about 3 MeV. Further, the 4343 keV level, which is weakly excited in (^{3}He, d) and shows a structureless angular distribution, is possibly one of the predicted $J^\pi \geq 4^+$ states around 4 MeV.

Spectroscopic strengths for the transitions to negative parity states (2^-, 3^-, 4^-) have also been calculated[22] by extending the calculations of Ref. 23 to include one particle in the $2p1f$ shell. The results are in good agreement for the lowest two 2^- states, but about a factor of 2 too large for the 3^- and 4^- states.

A deformed shell model with two particles distributed over the empty Nilsson orbits of a deformed mass 28 core has so far been used only to calculate energy levels and $B(E2)$ transition strength.[5] Further, a prolate deformation was assumed in these calculations and recent results on the quadrupole moment of ^{28}Si (2^+) suggest an oblate shape.[32]

The results of summing up all the G_j values with the restrictions discussed in Sec. IIIC are summarized in Table V. We find about the same number of $1d_{5/2}$ proton holes in the ^{28}Si and ^{29}Si targets. Because of the uncertainty in the absolute spectroscopic factors no significance can be attached to the small differences between the two sets of values. However, it appears quite clear

TABLE V. Summed proton transfer strengths for transitions to $2s1d$ and $1f2p$ orbitals.

	$\sum G_j$		
nlj	^{28}Si(^{3}He, d)^{29}P	^{29}Si(^{3}He, d)^{30}P	Sum rule limit [a]
$1d_{5/2}$	1.0	0.7	0
$2s_{1/2}$	1.3	1.4	2
$1d_{3/2}$	3.7	2.8	4
$1f_{7/2}$	3.7	3.7	8
$2p_{3/2}$	1.7	2.3	4
Total $2s1d$	6.0	4.9	6

[a] Assuming a filled $1d_{5/2}$ and empty $2s_{1/2}$, $1d_{3/2}$, $1f_{7/2}$, and $2p_{3/2}$ proton orbitals.

from Table V that the addition of the extra neutron to ^{28}Si does not alter the proton core significantly.

The total $2s1d$ strength is in good agreement with the shell model limit for both nuclei, but for the $1f_{7/2}$ and $2p_{3/2}$ orbits only half of the limit has been observed as we have mentioned already for the $1f_{7/2}$ orbit. It is quite possible, that the usual DWBA procedure needs to be modified for stripping to the next major shell ($2p1f$) beyond the valence nucleon shell ($2s1d$). However, it cannot be excluded that the missing $2p_{3/2}$ and $1f_{7/2}$ strength is contained in transitions to many higher lying states.

V. CONCLUSION

Simple two-particle features were observed for certain ^{30}P states. They were used to identify a number of states as isobaric analogs of ^{30}Si levels which are known from the ^{29}Si(d,p)^{30}Si reaction to have two-particle structure. Particularly striking examples are the $J^\pi = 3^-$ and 4^-, $T = 1$ states of the $(2s_{1/2})(1f_{7/2})$ configuration. The summed transition strength of all observed $l = 1$ and $l = 3$ transitions was found to be only one-half of the shell model limit for the $2p_{3/2}$ and $1f_{7/2}$ shells.

A large number of transitions to positive parity $T = 0$ and $T = 1$ states does exhaust almost all of the total $2s1d$ shell strength. The agreement between experimental G_j values and shell model predictions[23] is quite good for most positive parity states; however, the distribution of the $(2s_{1/2})^2$ strength among the many 1^+, $T = 0$ states is not reproduced by the shell model. The effects of truncating the full $2s1d$ shell model space are expected to be severe for the deformed nuclei in the middle of the $2s1d$ shell. However, the untruncated $2s1d$ shell model calculations[31] gave only fair agreement with experimental energy levels. This might point toward the need for a different effective interaction. It might also be necessary to consider explicitly excitations involving the $1p$ and $2p1f$ shells. In that case a description in a deformed shell model is perhaps more appropriate and a calculation of spectroscopic factors within the framework of that model would be of interest.

The authors are indebted to Dr. J. R. Erskine for permission to use the Argonne automatic plate scanning facility and to Dr. P. J. Ellis for a critical reading of the manuscript.

*Work supported in part by the Energy Research and Development Administration. This is report No. COO-1265-166.

[1]See M. Moinester, J. P. Schiffer, and W. P. Alford, Phys. Rev. 179, 984 (1969); J. P. Schiffer, Ann. Phys. (N.Y.) 66, 798 (1971).

[2]W. A. Lanford, W. P. Alford, and H. W. Fulbright, Bull. Am. Phys. Soc. 16, 493 (1971).

[3]N. Anantaraman and J. P. Schiffer, Phys. Lett. 37B, 229 (1971); J. P. Schiffer, in *The Two Body Force in Nuclei*, edited by S. M. Austin and G. M. Crawley (Plenum, New York, 1972).

[4]G. Mairle, Heidelberg, Report No. MPI-H-1972-V28 (unpublished).

[5]R. Ascuitto, D. A. Bell, and J. P. Davidson, Phys. Rev. 176, 1323 (1968); P. Wasielewski and F. B. Malik, Nucl. Phys. A160, 113 (1971), and references therein.

[6]H. Mackh, H. Oeschler, G. J. Wagner, D. Dehnhard, and H. Ohnuma, Nucl. Phys. A202, 497 (1973).

[7]P. Leleux, thesis, Université de Louvain, 1973 (unpublished); see also H. Ejiri, T. Ishimatsu, K. Yagi, G. Breuer, Y. Nakajima, H. Ohmura, T. Tohei, and T. Nakagawa, J. Phys. Soc. Jpn. 21, 2110 (1966).

[8]M. C. Mermaz, C. A. Whitten, Jr., J. W. Champlin, A. J. Howard, and D. A. Bromley, Phys. Rev. C 4, 1778 (1971).

[9]A. El-Naiem and R. Reif, Nucl. Phys. A189, 305 (1972); see also F. El-Bedewi and M. Shalaby, J. Phys. A5, 1624 (1972).

[10]P. D. Kunz (private communication).

[11]H. A. Enge, Nucl. Instrum. Methods 28, 126 (1964); J. E. Spencer and H. E. Enge, *ibid.* 49, 181 (1967).

[12]P. M. Endt and C. van der Leun, Nucl. Phys. A105, 1 (1967); A214, 1 (1973).

[13]P. Spink and J. R. Erskine, Argonne National Laboratory, Physics Division Informal Report No. PHY-1965B (unpublished); J. R. Comfort, Argonne National Laboratory Physics Division Informal Report No. PHY-1970B (unpublished).

[14]J. F. Sharpey-Schafer, P. R. Alderson, D. C. Bailey, J. L. Durell, M. W. Greene, and A. N. James, Nucl. Phys. A167, 602 (1971).

[15]P. J. Nolan, D. C. Bailey, P. E. Carr, L. L. Green,

A. N. James, J. F. Sharpey-Schafer, and D. A. Viggars, J. Phys. A5, 454 (1972).
[16]G. J. Pyle, J. H. Williams Laboratory of Nuclear Physics Informal Report No. COO-1265-64, Univ. of Minnesota (unpublished).
[17]B. H. Wildenthal and E. Newman, Phys. Rev. 167, 1027 (1968).
[18]A. W. Kuhfeld, J. H. Williams Laboratory of Nuclear Physics, Univ. of Minnesota, Annual Report, 1971 (unpublished), p. 190.
[19]B. Mertens, C. Mayer-Böricke, and H. Kattenborn, Nucl. Phys. A158, 97 (1970).
[20]R. H. Bassel, Phys. Rev. 149, 791 (1966).
[21]R. C. Hertzog, L. L. Green, M. W. Green, and G. D. Jones, J. Phys. A7, 72 (1974); see also M. W. Green, L. L. Green, and G. D. Jones, Phys. Lett. 32B, 680 (1970).
[22]J. Uzureau, D. Ardouin, and P. Avignon, Nucl. Phys. A230, 253 (1974).
[23]B. H. Wildenthal, private communication, also quoted in Ref. 22. For a description of the truncation scheme see B. H. Wildenthal and J. B. McGrory, Phys. Rev. C 7, 714 (1973).
[24]H. Mackh, G. Mairle, and G. J. Wagner, Z. Phys. 269, 353 (1974).
[25]T. T. S. Kuo and G. E. Brown, Nucl. Phys. A114, 241 (1968).
[26]G. I. Harris, A. K. Hyder, Jr., and J. Walinga, Phys. Rev. 187, 1413 (1969).
[27]J. P. Schiffer, in *Isospin in Nuclear Physics*, edited by D. H. Wilkinson (Univ. of Rochester, New York, 1968), Chap. 13; M. H. MacFarlane and J. B. French, Rev. Mod. Phys. 32, 567 (1960); J. B. French and M. H. MacFarlane, Nucl. Phys. 26, 168 (1961).
[28]D. Dehnhard, J. L. Artz, D. J. Weber, V. Shkolnik, and R. M. DeVries, Phys. Rev. C 13, 164 (1976).
[29]W. W. Dykoski and D. Dehnhard, Bull. Am. Phys. Soc. II 19, 554 (1974).
[30]B. M. Preedom and B. H. Wildenthal, Phys. Rev. C 6, 133 (1972).
[31]B. J. Cole, A. Watt, and R. R. Whitehead, J. Phys. A7, 1374 (1974).
[32]D. Schwalm, A. Bamberger, P. G. Bizzeti, B. Povh, G. A. P. Engelbertink, J. W. Olness, and E. K. Warburton, Nucl. Phys. A192, 449 (1972).